SCIENTIFIC REPORTS
nature research

OPEN

Effect of asymmetrical heat rise/fall on the film flow of magnetohydrodynamic hybrid ferrofluid

Iskander Tlili[1,2], M. T. Mustafa[3], K. Anantha Kumar[4*] & N. Sandeep[5*]

The movement of the ferrous nanoparticles is random in the base fluid, and it will be homogeneous under the enforced magnetic field. This phenomenon shows a significant impact on the energy transmission process. In view of this, we inspected the stream and energy transport in magnetohydrodynamic dissipative ferro and hybrid ferrofluids by considering an uneven heat rise/fall and radiation effects. We studied the Fe_3O_4 (magnetic oxide) and $CoFe_2O_4$ (cobalt iron oxide) ferrous particles embedded in H_2O-EG (ethylene glycol) (50–50%) mixture. The flow model is converted as ODEs with suitable similarities and resolved them using the 4th order Runge-Kutta scheme. The influence of related constraints on transport phenomena examined through graphical illustrations. Simultaneous solutions explored for both ferro and hybrid ferrofluid cases. It is found that the magnetic oxide and cobalt iron oxide suspended in H_2O-EG (ethylene glycol) (50–50%) mixture effectively reduces the heat transfer rate under specific conditions.

The fluid flows across a stretching surface have attained plentiful implications in the analysis of boundary layer flow owing to its great solicitations in medical, industrial, and mechanical engineering applications. Food dispensation, silicon wafer process, hot rolling, cooling of reactors, design of precious stone, tinning of wires, continuous casting of metals, paper production, making of microchips, glass industry, crystal growth, space vehicles, polymer physics are some applications of such motion in a time-dependent liquid film flow across a surface. Anderson *et al.*[1] discussed the problem of liquid film movement of a Newtonian fluid through a strained surface. The influence of radiative heat and variable thermal conductivity on shear thickening fluid drive of a liquid film on the unsteady permeable extending superficial inspected by Khan *et al.*[2] and Shah *et al.*[3] It clinched that the distribution of heat and the variable temperature parameter are linearly proportional beside the surface. Idrees *et al.*[4] studied an elucidation of the problem of an unsteady MHD thin-film flow owing to stressed sheet in the appearance of mutable viscosity. Recently, Kumar *et al.*[5] bestowed dual elucidations for micropolar conducting fluid flow past an overextended sheet in the presence of second-order velocity slip.

The frictional heat mechanism has an active role in industrial and scientific implications such as electric coffee fabricators, rock forms, cuisine diet, and sanitization. Chen[6] considered a problem of an unsteady two-dimensional shear-thickening film flow over an elongated geometry to examine the influence of viscous dissipation. Later, Chen[7] extended the problem with Joule's heat and gave a result with the support of the numeric Keller-Box scheme. The effect of frictional heat on the natural convective 2D drive of hybrid nano liquid over a circular tube was discussed by Suresh *et al.*[8] Numerical scrutiny was accompanied by Ramandevi *et al.*[9] for the comparison of the heat transfer mechanism in both viscoelastic and Casson fluid flow using new heat flux under the action of and viscous dissipation. Recently, the authors[10] discussed the impact of Joule heating on fluid motion owing to the extending sheet in the occurrence of Biot number.

Newly, scientists and researchers made an immense effort to examine the significance and separation of hybrid ferrofluids due to their applications in many branches of natural, engineering, and physical sciences. A magnetic

[1]Department for Management of Science and Technology Development, Ton Duc Thang University, Ho Chi Minh City, Vietnam. [2]Faculty of Applied Sciences, Ton Duc Thang University, Ho Chi Minh City, Vietnam. [3]Department of Mathematics, Statistics and Physics, Qatar University, Doha, 2713, Qatar. [4]Department of Mathematics, Sri Venkateswara University, Tirupati, 517502, India. [5]Department of Mathematics, Central University of Karnataka, Kalaburagi, 585367, India. *email: ananth.svu@gmail.com; nsandeep@cuk.ac.in

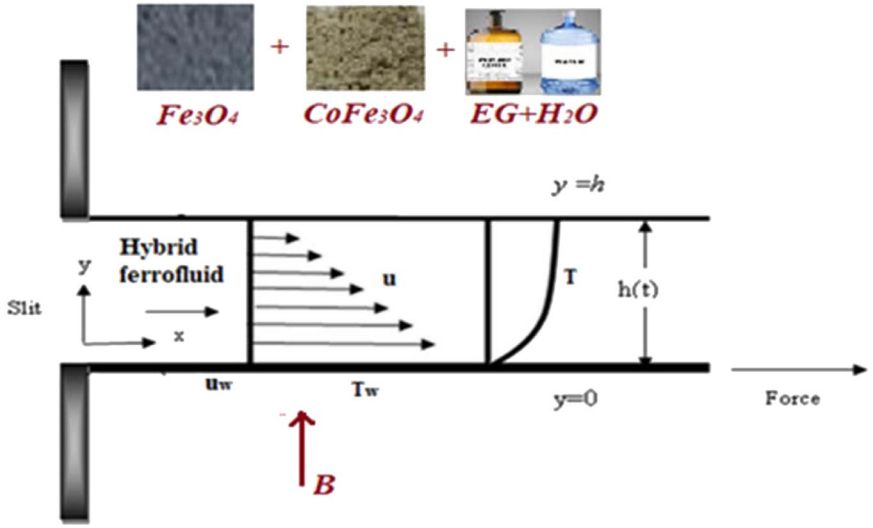

Figure 1. Flow configuration.

colloid is well-known as a ferrofluid. A ferrofluid is a colloidal interruption of single-domain ferromagnetic elements in a base liquid. It has several medicinal and biological solicitations like amplifiers, revolving shaft seals, vacuum chambers, computer drives, dissipation of radiation, medicine delivery, cell parting, etc. A nanofluid consists of a single nanomaterial, whereas the hybrid nanofluid consists of more than one unlike nanoparticles with ordinary fluid. The determination behind the invention of a mixture of ferrofluids is to knob the transport phenomena. Madhesh and Kalaiselvam[11] discussed the rheological appearances and temperature transmission of hybrid nanofluids. The magnetohydrodynamic time-dependent liquid film flow of grapheme nanoparticles embedded nanofluid under various thermal transport aspects can be viewed in ref. [12] The influence of drag force on the flow over an expanding surface was discussed by Sheikholeslami *et al.*[13] Later on, the researchers[14,15] investigated the transport phenomena of Newtonian and non-Newtonian hybrid nanoliquids under various physical effects. Kumar *et al.*[16] discussed the effect of Brownian moment on bio convective stagnated motion of nanoliquid and presented dual solutions. It was clinched that the measure of thermal transport is high in the case of hybrid nanofluid when matched with another liquid. Sandeep[17] deliberated the influence of drag force and variable viscosity on the hybrid nanofluid drive of liquid film over a fraught sheet.

The inspiration for radiating heat on convective movements shows a massive role in many engineering and scientific procedures like space technology, paper bowls production, freezing of metal bits, satellites, design of electronic chips, and fuel wells. The radiation is either or nonlinear depends on temperature ratio parameter values. The mechanism of asymmetrical heat rise or fall has well-known uses in drug industries and numerous manufacturing happenings like freezing of metal strips and crude oil recovery, etc. Devi and Devi[18] considered a problem to investigate a numerical explanation for MHD flow of nanoliquid across a penetrable sheet with heat rise/fall. Kandelousi and Ellahi[19] scrutinized a time-independent, two-dimensional ferrohydrodynamic flow through a square cavity in the occurrence of drag force. The well-known Lattice Boltzmann technique is utilized to resolve the equations of motion. Afrand *et al.*[20] contemplated a problem to examine the Power-law fluid. The stimulus of radiation on the hydrodynamic drive of shear thickening over a stretched surface was scrutinized by Ramzan *et al.*[21] Ghadikolaei[22] deliberated the magnetohydrodynamic free convective motion of two different hybrid nanofluids across an overextended surface. The impact of thermic heat on MHD flow of micropolar shear-thickening nanoliquid thru a nonlinear stretched sheet was examined by Lu *et al.*[23] numerically with the help of the Matlab package. Kumar *et al.*[24] discussed the inspiration of asymmetrical heat generation or absorption and nonlinear thermic heat on slanting stagnated motion of shear thickening fluid across a vertical sheet in conducting field. The impact of non-linear thermal radiation and resistive heating on MHD shear-thickening nanoliquid flow over an inclined penetrable stretched sheet was reported by Ghadikolaei *et al.*[25] Discrete heating effect on free convection flow past a vertical annulus was studied by the researchers[26–29]. Sankar *et al.*[30] performed a numerical investigation to analyze the heat and mass transfer rates in the presence of discrete heat source.

In all the afford studies, scientists scrutinized the transport phenomena of nanoliquids past a solid geometry with numerous physical aspects. The main motto of this exploration is to provide a numerical examination of the stream and energy transport in magnetohydrodynamic dissipative ferro and hybrid ferrofluids by considering an uneven heat rise/fall and radiation effects. We studied the Fe_3O_4 (magnetic oxide) and $CoFe_2O_4$ (cobalt iron oxide) ferrous particles embedded in H_2O-EG (ethylene glycol) (50–50%) mixture. The flow model is converted as ODEs with suitable similarities and resolved them using the 4th order Runge-Kutta scheme. The influence of related constraints on transport phenomena examined through graphical illustrations. Simultaneous solutions are explored for both ferrous and hybrid ferrofluid cases.

Property	ρ(Kg/m^3)	c_p(J/KgK)	k(W/mK)	σ(S/m)
H_2O + EG(50%−50%)	1057	3287	0.424	0.005
Magnetic oxide	5180	670	9.8	0.74×10^6
Cobalt iron oxide	4908	700	3.6	1.1×10^7

Table 1. Thermophysical possessions.

S	Xu *et al.*[26]	Sandeep *et al.*[12]	Current Results
1.0	2.67722	2.67722	2.677224531
1.2	1.99959	1.99959	1.999593210
1.4	1.44775	1.44775	1.447752761
1.6	0.95669	0.95669	0.956693254

Table 2. Authentication of the outputs of $-\theta'(0)$ when $\Pr = 1,\ M = \phi = Ec = R = 0$.

Modelling

Consider a time dependent flow of EG-H_2O based magnetic and cobalt iron oxide mixture hybrid ferrofluid past an extending sheet as depicted in Fig. 1. Here, the surface is placed lengthways x-axis with the temperature and momentum respectively taken as $T_w = T_0 - T_{re}\sqrt{b^2x^4/4\nu_f^2\left(1-\alpha t\right)}$, $0 \le T_{re} \le T_0$, and $u_w = bx/(1-\alpha t)$ and y - axis is normal to it (where b, α are constants and T_0, T_{re} are slit, reference temperatures)

An electromagnetic field of forte $B = B_0\sqrt{1/(1-\alpha t)}$ is measured normal to the drive. Thermal radiation, asymmetrical heat rise/fall and viscous dissipation possessions are engaged. The slip between the particles is neglected. With the above conventions, the leading transport equalities are as follows:

$$\frac{\partial u}{\partial x} + \frac{\partial v}{\partial y} = 0, \tag{1}$$

$$u\frac{\partial u}{\partial x} + v\frac{\partial u}{\partial y} + \frac{\partial u}{\partial t} = \frac{\mu_{hnf}}{\rho_{hnf}}\frac{\partial^2 u}{\partial y^2} + \frac{\sigma_{hnf}}{\rho_{hnf}}B^2u, \tag{2}$$

$$u\frac{\partial T}{\partial x} + v\frac{\partial T}{\partial y} + \frac{\partial T}{\partial t} = \frac{k_{hnf}}{(\rho c_p)_{hnf}}\frac{\partial^2 T}{\partial y^2} + \frac{1}{(\rho c_p)_{hnf}}\frac{16T_\infty^3\sigma^*}{3k^*}\frac{\partial^2 T}{\partial y^2} + \mu_{hnf}\left(\frac{\partial u}{\partial y}\right)^2 + q''', \tag{3}$$

Frontier limitations:

$$\begin{aligned} &u(0) = u_w,\ T(0) = T_w,\ v(0) = 0,\ \text{and} \\ &u_y(h) = T_y(h) = 0\ ,\ v = h_t\ at\ y = h(t), \end{aligned} \tag{4}$$

where

$$q''' = \frac{k_f b}{(1-\alpha t)\nu_f}(A^*(T_w - T_0)f' + (T - T_0)B^*), \tag{5}$$

where, the dynamic viscosity, density, electrical conductivity, thermal conductivity, specific heat capacitance, Stefan–Boltzmann constant, uneven heat source/sink parameters and radiative absorption coefficient are respectively given by μ, ρ, σ, k, c_p, σ^*, A^*, B^* *and* k^*. Here, the suffix *nf* and *hnf* denotes the nano and hybrid nanoliquid.

Similarity transmutations[26]

$$\left.\begin{aligned} &\eta = \sqrt{\frac{by^2}{\beta^2\nu_f(1-\alpha t)}},\ \psi = \sqrt{\frac{\beta^2\nu_f bx^2}{(1-\alpha t)}}f(\eta),\ \theta = \frac{(T-T_0)}{(T_w-T_0)}, \\ &u = \psi_y,\ v = -\psi_x,\ T_w = T_0 - T_{re}\sqrt{b^2x^4/4\nu_f^2(1-\alpha t)^3}\,\theta(\eta), \end{aligned}\right\} \tag{6}$$

The ferrofluid restrictions are taken as

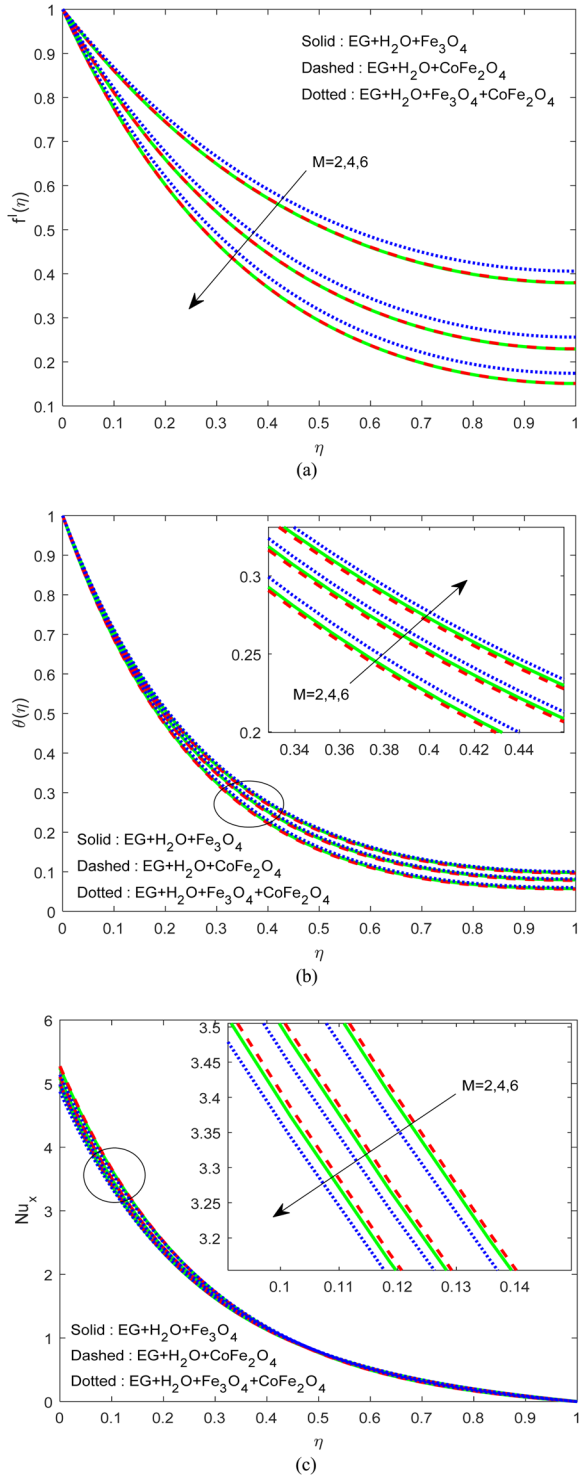

Figure 2. Variation of M on (**a**) Flow (**b**) Energy (**c**) Nu_x.

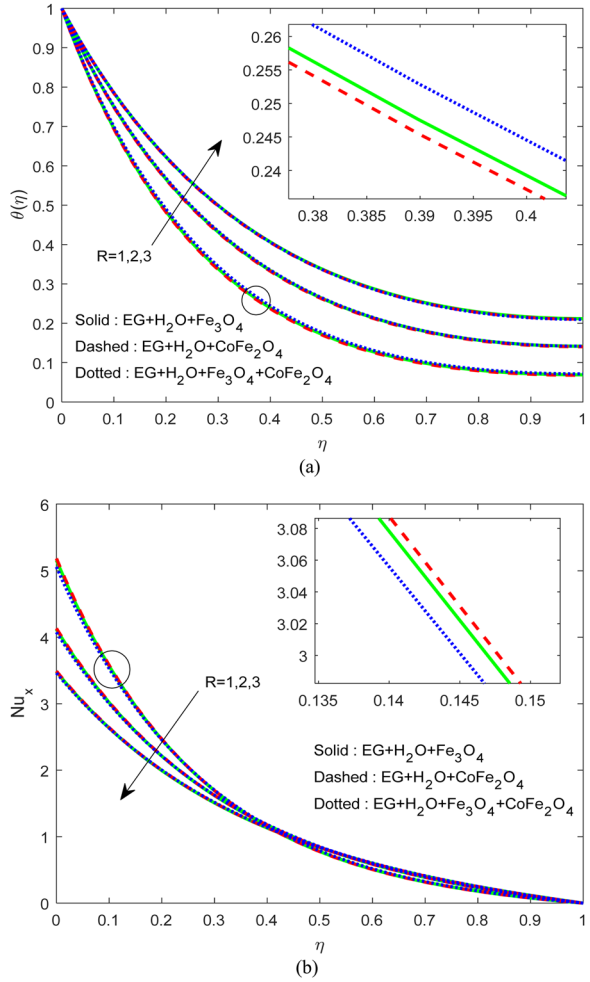

Figure 3. Variation of R on (**a**) Flow (**b**) Nu_x.

$$\left.\begin{aligned}
&\frac{k_{hnf}}{k_f} = \frac{k_{2s} + 2k_f - 2\phi_2(k_f - k_{2s})}{k_{2s} + 2k_f + \phi_2(k_f - k_{2s})} \times k_{nf},\ k_{nf} = \frac{k_{1s} + 2k_f - 2\phi_1(k_f - k_{1s})}{k_{1s} + 2k_f + \phi_1(k_f - k_{1s})},\\
&\frac{\rho_{hnf}}{\rho_f} = (1-\phi_2)\left[(1-\phi_1) + \frac{\phi_1\rho_{1s}}{\rho_f}\right] + \frac{\phi_2\rho_{2s}}{\rho_f},\ \frac{\mu_{hnf}}{\mu_f} = \frac{1}{(1-\phi_1)^{2.5}(1-\phi_2)^{2.5}},\\
&\frac{(\rho c_p)_{hnf}}{(\rho c_p)_f} = (1-\phi_2)\left[(1-\phi_1) + \frac{\phi_1(\rho c_p)_{1s}}{(\rho c_p)_f}\right] + \frac{\phi_2(\rho c_p)_{2s}}{(\rho c_p)_f},\\
&\frac{\sigma_{hnf}}{\sigma_f} = \left[1 + \frac{3(\sigma_{1s}\phi_{1s} - \phi\sigma_f) + \phi_{2s}\sigma_{2s}}{\sigma_{1s}(1-\phi_{1s}) + \sigma_{2s}(1-\phi_{2s}) + (2+\phi)\sigma_f}\right],\ \phi = \phi_1 + \phi_2,
\end{aligned}\right\} \tag{7}$$

Using Eqs. (5) to (7), the Eqs. (2) to (4) can be distorted as

$$\left.\begin{aligned}
&\frac{1}{(1-\phi_1)^{2.5}(1-\phi_2)^{2.5}} f''' + \left\{(1-\phi_2)\left((1-\phi_1) + \frac{\phi_1\rho_{1s}}{\rho_f}\right) + \frac{\phi_2\rho_{2s}}{\rho_f}\right\}\\
&\times\lambda(f'' - Sf' - f'^2 - 0.5S\eta f'')\\
&-M\left[1 + \frac{3(\sigma_{1s}\phi_{1s} - \phi\sigma_f) + \phi_{2s}\sigma_{2s}}{\sigma_{1s}(1-\phi_{1s}) + \sigma_{2s}(1-\phi_{2s}) + (2+\phi)\sigma_f}\right]f' = 0,
\end{aligned}\right\} \tag{8}$$

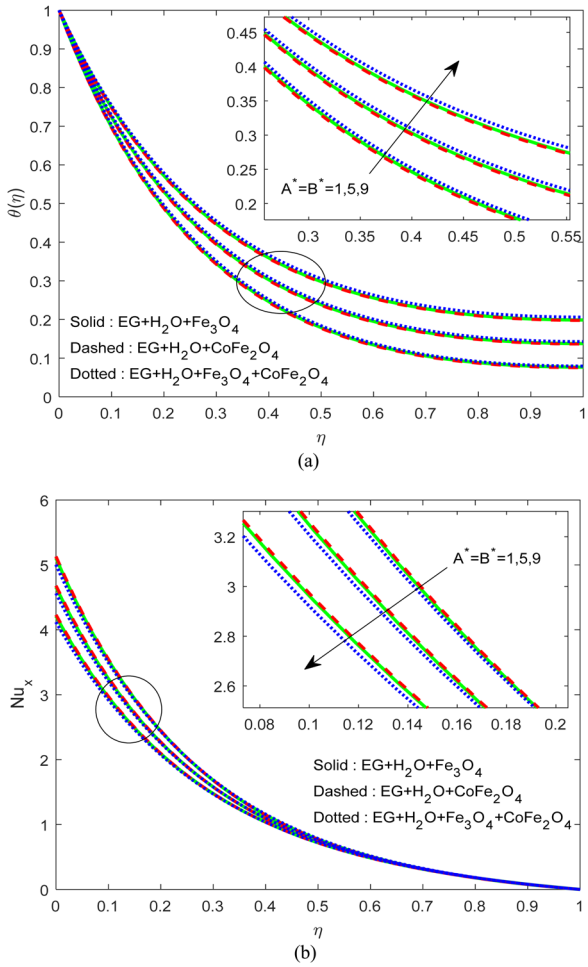

Figure 4. Variation of A^* & B^* on (**a**) flow (**b**) Nu_x.

$$\left.\begin{aligned}&\left(\frac{k_{2s}+2k_f-2\phi_2(k_f-k_{2s})}{k_{2s}+2k_f+\phi_2(k_f-k_{2s})}\times k_{nf}+\frac{4}{3}R\right)\theta''+\mathrm{Pr}Ecf''^2+B^*\theta+A^*f'\\&-\mathrm{Pr}\left((1-\phi_2)\left((1-\phi_1)+\frac{\phi_1(\rho c_p)_{1s}}{(\rho c_p)_f}\right)+\frac{\phi_2(\rho c_p)_{2s}}{(\rho c_p)_f}\right)\lambda(2f'\theta 0.5S(3\theta+\eta\theta')-f\theta')=0,\end{aligned}\right\} \tag{9}$$

Transformed boundaries:

$$\begin{aligned}&f(\eta)=0,\ \theta(\eta)=1,f'(\eta)=1,at\ \eta=0,\\&f(1)=0.5S,\ \left.\frac{\partial^2 f}{\partial\eta^2}\right|_{\eta=1}=0,\ \left.\frac{\partial\theta}{\partial\eta}\right|_{\eta=1}=0,\end{aligned} \tag{10}$$

where, ϕ_1, ϕ_2 denotes the nanoparticle volume fraction and the suffixes f, s denotes the fluid and solid particles. And the dimensionless magnetic field parameter, Prandtl number, Radiation parameter, Unsteadiness parameter, Eckert number and film thickness quantities are specified by

$$M=\frac{\sigma_f B_0^2}{b\rho_f},\ \mathrm{Pr}=\frac{\nu_f}{\alpha_f},\ R=\frac{4\sigma^* T_0^3}{k^* k_f},\ S=\frac{\alpha}{b},\ Ec=\frac{u_w^2}{(c_p)_f(T_w-T_0)},\ \lambda=\beta^2, \tag{11}$$

The reduced Nusselt number Nu_x is specified as

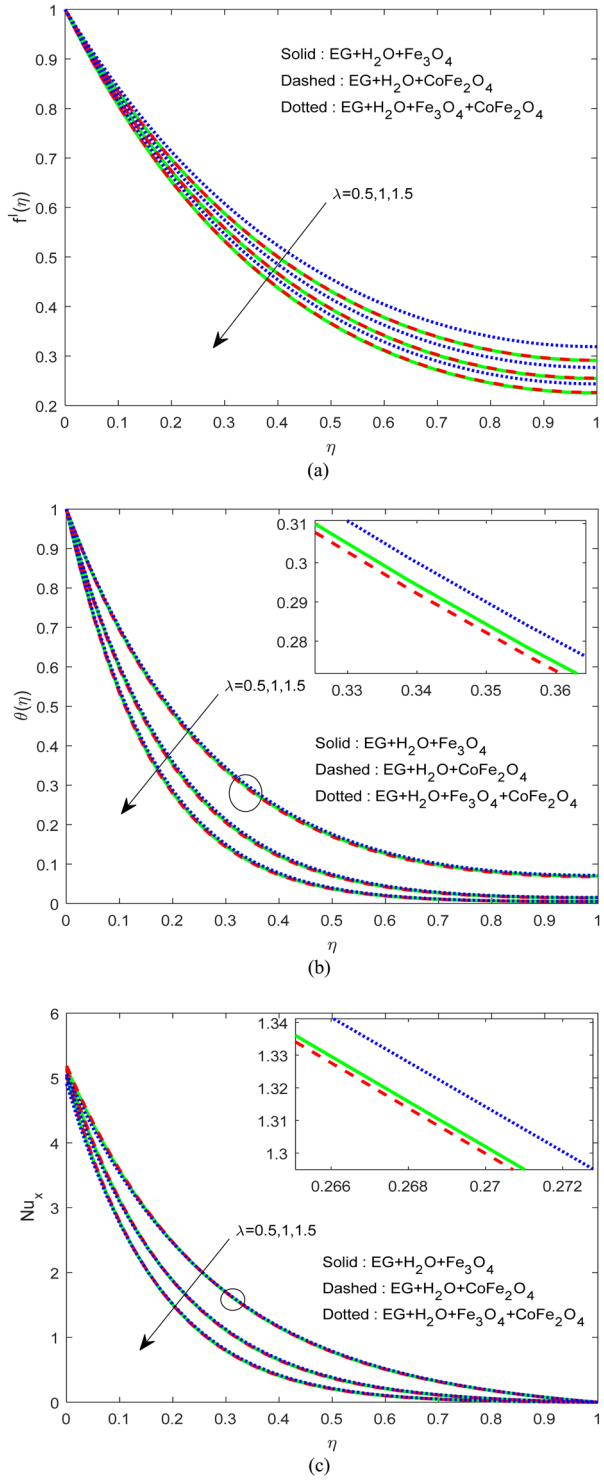

Figure 5. Variation of λ on (**a**) Flow (**b**) Energy (**c**) Nu_x.

$$Nu_x = -\beta^{-1}\mathrm{Re}_x^{1/2}\left(\frac{k_{2s} + 2k_f - 2\phi_2(k_f - k_{2s})}{k_{2s} + 2k_f + \phi_2(k_f - k_{2s})} \times k_{nf} + 1.33R\right)\theta'(0), \tag{12}$$

with the Reynolds number $\mathrm{Re}_x = \frac{u_w x}{\nu_f}$.

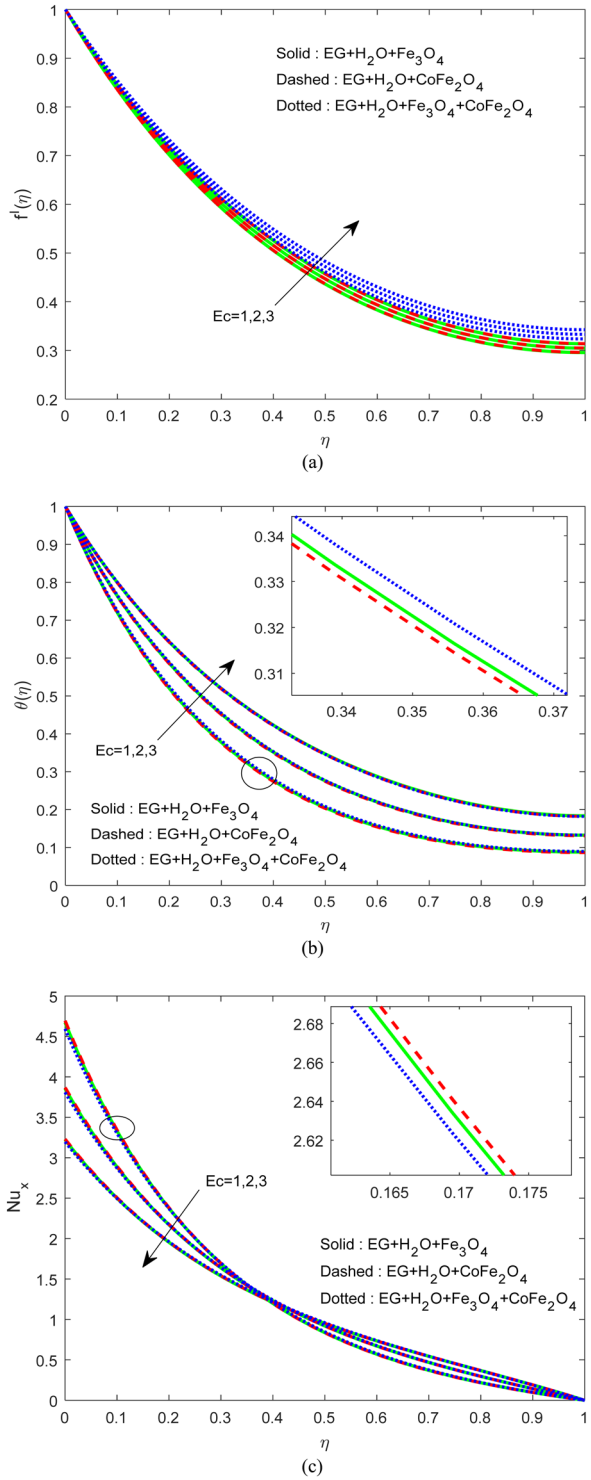

Figure 6. Variation of *Ec* on (**a**) Flow (**b**) Energy (**c**) Nu_x.

Results and Discussion

The Eqs. (8) and (9) with the constraints in Eq. (10) are resolved by the RK-shooting scheme. The assets of non-dimensional restrictions on the drive, energy fields along with Nusselt number are elucidated explicitly. The results are displayed for (H_2O-EG-Fe_3O_4) water-EG-magnetic oxide ferrofluid (solid lines), (H_2O-EG-$CoFe_2O_4$) water-EG-cobalt iron oxide ferrofluid (dashed lines) and water-EG- magnetic/cobalt iron oxide hybrid ferrofluid (dotted lines) cases. For computing purpose, the dimensionless quantities can be considered as $M = 3$, $R = 1$, $\phi_1 = \phi_2 = 0.1$; $Ec = S = \lambda = A^* = B^* = 0.5$, $\mathrm{Pr} = 30$. Table 1 predicts the physical properties, and Table 2 discusses the authentication of the outputs.

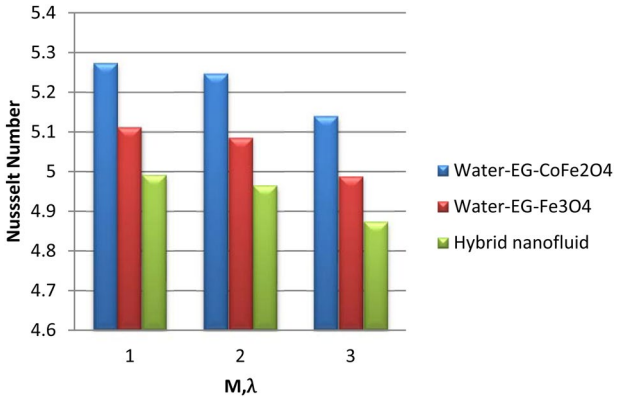

Figure 7. Variation of M, λ on Nu_x.

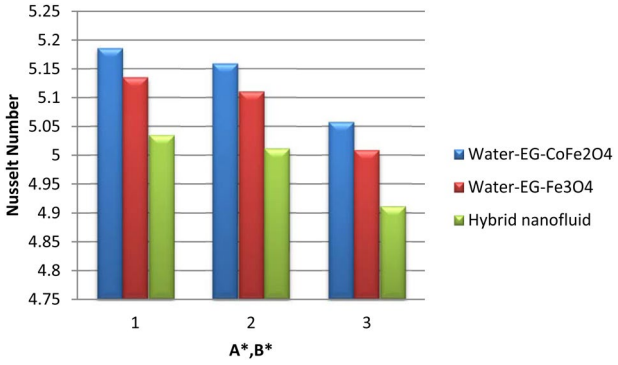

Figure 8. Variation of A^*, B^* on Nu_x.

Figure 2 explains the impression of M on the drive and thermal fields along with Nusselt number. The momentum boundary layer of water-EG-magnetic/cobalt iron oxide hybrid ferrofluid is less influenced by M when equated with water-EG-magnetic oxide and water-EG-cobalt iron oxide ferrofluids. And the opposite trend has been noticed in the thermal boundary layer as displayed in Fig. 2(a). The reason for these trends is the drag force developed against the flow due to the imposing of external magnetic force. As a rise in the resultant temperature, we noticed a fall in the Nusselt number, as shown in Fig. 2(c). Notably, it is less in H_2O-EG-Fe_3O_4/$CoFe_2O_4$ hybrid ferrofluid when compared to other two ferrofluids.

Figure 3 explicate the influence of R and uneven heat rise/fall on $\theta(\eta)$ and Nu_x. As per the general nature of R, A^* and B^*, a rise in the heat input primes to upsurge in the heat field. A similar drift was followed by Fig. 4. However, we observed a significant hike in the thermal field of H_2O-EG-Fe_3O_4/$CoFe_2O_4$ hybrid ferrofluid when compared to the other two ferrofluids. These may be due to the enhanced heat conduction between the Fe_3O_4-$CoFe_2O_4$ solid particles. As a result, we found decay in Nu_x in all cases for growing numbers of R, A^* and B^* (see Figs. 3(b) and 4(b)).

Figure 5 expounds the result of λ on $f'(\eta)$, $\theta(\eta)$ and Nu_x. We perceived a depreciation in momentum and thermal arenas for boosting values of λ. Notably, we noticed that the impact of λ is high on the thermal filed of H_2O-EG-$CoFe_2O_4$ ferrofluid when equated to water-EG-magnetic oxide ferrofluid and water-EG-magnetic/cobalt iron oxide hybrid ferrofluid. Generally, a rise in the film thickness leads to enlarging the flow filed and hence reduces the heat transfer. Cobalt may be the reason for the additional reduction in the heat transfer of H_2O-EG-$CoFe_2O_4$ ferrofluid.

Figure 6 illustrate the control of viscous dissipation on $f'(\eta)$, $\theta(\eta)$ and Nu_x. It is profound that the growing values of Ec effectively escalate the thermal and drive boundary layers. Physically, drive force can be converted as heat energy in viscous fluids. If the viscosity of the fluid is high, then more internal heat energy will generate and hence the heat transfer. Interestingly, enhancing the fluid viscosity commendably enhancing the flow and thermal fields of H_2O-EG-Fe_3O_4/$CoFe_2O_4$ hybrid ferrofluid when equated to the other two ferrofluids. Figures 7 and 8 exemplify the impression of M, λ, A^* and B^* on Nusselt number. It is evident that the boosting standards of M, λ, A^* and B^* decline the heat transfer rate in all cases. Mainly, this influence is high on H_2O-EG-Fe_3O_4/$CoFe_2O_4$ hybrid ferrofluid.

Conclusions

Due to the numerous applications of ferrofluid fluids in the heat transfer process, a computational analysis is performed to investigate the drive and heat transport in EG-H2O/Fe3O4 ferroliquid, water-EG/CoFe2O4 ferroliquid and water-EG-magnetic oxide/cobalt iron oxide ferrofluid hybrid ferrofluid in the presence of thermal radiation, dissipation and uneven energy generation/fall. Observations of the current analysis are listed below:

- The drive of water-EG-magnetic oxide/cobalt iron oxide hybrid ferrofluid is effectively controlled by M.
- Thermal radiation and asymmetrical heat rise/fall regulates the energy transport in H_2O-EG-Fe_3O_4/$CoFe_2O_4$ hybrid ferrofluid.
- Enhancement in film thickness and addition of cobalt leads to a gradual decline in the thermal boundary layer thickness.
- $CoFe_2O_4$ may works like an insulator by increasing the concentration of cobalt.
- H_2O-EG-Fe_3O_4/$CoFe_2O_4$ hybrid ferrofluid may be used as a coolant by balancing the cobalt levels.
- By monitoring the viscous levels, we can control the internal heat transfer of H_2O-EG-Fe_3O_4/$CoFe_2O_4$ hybrid ferrofluid.

Received: 29 January 2019; Accepted: 30 March 2020;
Published online: 21 April 2020

References

1. Anderson, H. I., Aarseth, J. B. & Dandpat, B. S. Heat transfer in a liquid film on an unsteady stretching surface. *Int. Heat Mass Transf* **43**, 69–74 (2000).
2. Khan, Y., Wu, Q., Faraz, N. & Yildirim, A. The effects of variable viscosity and thermal conductivity on a thin film flow over a shrinking/stretching sheet. *Comp. Math. Appl.* **61**, 3391–3399 (2011).
3. Shah, Z., Bonyah, E., Islam, S., Khan, W. & Ishaq, M. Radiative MHD thin film flow of Williamson fluid over an unsteady permeable stretching sheet. *Heliyon* **4**, e00825 (2018).
4. Idrees, M., Rehman, S., Shah, R. A., Ullah, M. & Abbas, T. A similarity solution of time dependent MHD liquid film flow over stretching sheet with variable physical properties. *Res. Phys* **8**, 194–205 (2018).
5. Kumar, K. A., Sugunamma, V., Sandeep, N. & Mustafa, M. T. Simultaneous solutions for first order and second order slips on micropolar fluid flow across a convective surface in the presence of Lorentz force and variable heat source/sink. *Sci. Rep.* **9**, 14706 (2019).
6. Chen, C. H. Effect of viscous dissipation on heat transfer in a non-Newtonian liquid film over an unsteady stretching sheet. *J. Non-Newt. Fluid Mech* **135**, 128–135 (2006).
7. Chen, C. H. Combined effects of Joule heating and viscous dissipation on magnetohydrodynamic flow past a permeable stretching surface with free convection and radiative heat transfer. *J. Heat Transf* **132**, 064503 (2010).
8. Suresh, S., Venkitaraj, K. P., Selvakumar, P. & Chandrasekar, M. Effect of Al_2O_3-Cu/water hybrid nanofluid in heat transfer. *Exp. Therm. Fluid Sci.* **38**, 54–60 (2012).
9. Ramandevi, B., Reddy, J. V. R., Sugunamma, V. & Sandeep, N. Combined influence of viscous dissipation and non-uniform heat source/sink on MHD non-Newtonian fluid flow with Cattaneo-Christov heat flux. *Alex. Eng. J* **57**, 1009–1018 (2018).
10. Srinivasacharya, D. & Jagadeeshwar, P. Effect of Joule heating on the flow over an exponentially stretching sheet with convective thermal condition. *Math. Sci* **13**, 201–2011 (2019).
11. Madhesh, D. & Kalaiselvam, S. Experimental study on heat transfer and rheological characteristics of hybrid nanofluids for cooling applications. *J. Exp. Nanosci.* **10**(15), 1194–1213 (2015).
12. Sandeep, N. & Malvandi, A. Enhanced heat transfer in liquid thin film flow of non-Newtonian nanofluids embedded with graphene nanoparticles. *Adv. Powder Tech* **27**, 2448–2456 (2016).
13. Sheikholeslami, M., Mustafa, M. T. & Ganji, D. D. Effect of Lorentz forces on forced-convection nanofluid flow over a stretched surface. *Particuology* **26**, 108–113 (2016).
14. Afridi, M. I., Tlili, I., Goodarzi, M., Osman, M. & Khan, N. A. Irreversibility Analysis of Hybrid Nanofluid Flow over a Thin Needle with Effects of Energy Dissipation. *Symmetry* **11**, 663 (2019).
15. Subhani, M. & Nadeem, S. Numerical investigation of unsteady MHD flow of micropolar hybrid nanofluid in porous medium, *Physica Scripta*, **94**, https://doi.org/10.1088/1402-4896/ab154a (2019).
16. Kumar, K., Sugunamma, V., Sandeep, N. & Reddy, J. V. R. Impact of Brownian motion and thermophoresis on bio-convective flow of nanoliquids past a variable thickness surface with slip effects. *Mult. Mod. in Mat. and Stru* **15**, 103–132 (2018).
17. Sandeep, N. Effect of aligned magnetic field on liquid film flow of magnetic-nanofluid embedded with graphene nanoparticles. *Adv. Powder Tech.* **28**, 865–875 (2017).
18. Devi, S. P. A. & Devi, S. S. U. Numerical Investigation of Hydromagnetic Hybrid Cu – Al_2O_3/Water Nanofluid Flow over a Permeable Stretching Sheet with Suction. *Int. J. Nonlinear Sci. Numer. Simul* **17**, 149–257 (2016).
19. Kandelousi, M. S. & Ellahi, R. Simulation of ferrofluid flow for magnetic drug targeting using the lattice Boltzmann method. *Zeitschrift für Naturforschung A* **70**, 115–124 (2015).
20. Afrand, M., Oghraie, D. & Ruhani, B. Effects of temperature and nanoparticles concentration on rheological behavior of Fe3O4–Ag/EG hybrid nanofluid: an experimental study. *Exp.Ther. and Fluid Sci.* **77**, 38–44 (2016).
21. Ramzan, M., Ullah, N., Chung, J. D., Lu, D. & Farooq, U. Buoyancy effects on the radiative magneto Micropolar nanofluid flow with double stratification, activation energy and binary chemical reaction. *Sci. Rep.* **7**, 12901 (2017).
22. Ghadikolaei, S. S., Yassari, M., Sadeghi, H., Hosseinzadeh & Ganji, D. D. Investigation on thermophysical properties of Tio2–Cu/H2O hybrid nanofluid transport dependent on shape factor in MHD stagnation point flow. *Powder Tech.* **322**, 428–438 (2017).
23. Lu, D., Ramzan, M., Ahmad, S., Chung, J. D. & Farooq, U. A numerical treatment of MHD radiative flow of Micropolar nanofluid with homogeneous-heterogeneous reactions past a nonlinear stretched surface. *Sci. Rep.* **8**, 12431 (2018).
24. Kumar, K. A., Sugunamma, V. & Sandeep, N. Impact of non-linear radiation on MHD non-aligned stagnation point flow of micropolar fluid over a convective surface. *J. Non-Equilib. Thermo.* **43**, 327–345 (2018).
25. Ghadikolaei, S. S., Hosseinzadeh, K., Ganji, D. D. & Jafari, B. Nonlinear thermal radiation effect on magneto Casson nanofluid flow with Joule heating effect over an inclined porous stretching sheet. *Case Stud. in Ther. Eng.* **12**, 176–187 (2018).
26. Xu, H., Pop, I. & You, X. Flow and heat transfer in a nano-liquid film over an unsteady stretching surface. *Int. J. Heat Mass Transf* **60**, 646–652 (2013).
27. Sankar, M., Park, Y., Lopez, J. M. & Do, Y. Numerical study of natural convection in a vertical porous annulus with discrete heating. *Int. J. Heat Mass Transf* **54**, 1493–1505 (2011).

28. Sankar, M. & Do, Y. Numerical simulation of free convection heat transfer in a vertical annular cavity with discrete heating. *Int. Comm. Heat Mass Transf* **37**, 600–606 (2010).
29. Sankar, M. & Park, J. Younghae Do. Natural convection in a vertical annuli with discrete heat sources. *Num. Heat Transfer, Part A: Applications* **59**, 594–615 (2011).
30. Sankar, M., Beomseok, K., Lopez, J. M. & Do, Y. Thermosolutal convection from a discrete heat and solute source in a vertical porous annulus. *Int. J. Heat Mass Transf.* **55**, 4116–4128 (2012).

Acknowledgements
Authors acknowledge the UGC-India for start-up grant No. 30-489/2019(BSR).

Author contributions
I.T. explored the graphical results, K.A. did the literature survey, N.S. formulated the problem and explored the results. M.T.M discussed the results. All authors look over the final script and approved.

Competing interests
The authors declare no competing interests.

Additional information
Correspondence and requests for materials should be addressed to K.A.K. or N.S.

Reprints and permissions information is available at www.nature.com/reprints.

Publisher's note Springer Nature remains neutral with regard to jurisdictional claims in published maps and institutional affiliations.